

Efficient membrane element for cyclic response of RC panels

Lepoldo Tesser^{1a} and Diego A. Talledo^{*2}

¹*Géodynamique & Structure, 106, Avenue Marx Dormoy, 82120, Montrouge, France*

²*Department of Architecture Construction Conservation (DACC), University IUAV of Venice, Campus Terese, Dorsoduro 2206, 30123, Venice, Italy*

(Received January 17, 2017, Revised April 21 2017, Accepted May 10, 2017)

Abstract. This paper presents an efficient membrane finite element for the cyclic inelastic response analysis of RC structures under complex plane stress states including shear. The model strikes a balance between accuracy and numerical efficiency to meet the challenge of shear wall simulations in earthquake engineering practice. The concrete material model at the integration points of the finite element is based on damage plasticity with two damage parameters. All reinforcing bars with the same orientation are represented by an embedded orthotropic steel layer based on uniaxial stress-strain relation, so that the dowel and bond-slip effect of the reinforcing steel are presently neglected in the interest of computational efficiency. The model is validated with significant experimental results of the cyclic response of RC panels with uniform stress states.

Keywords: reinforced concrete panel; reinforced concrete membrane; inelastic cyclic analysis; finite element analysis

1. Introduction

Reinforced concrete (RC) shear walls are widely used either alone or in connection with moment resisting frames to meet lateral strength and ductility requirements for structures in zones of moderate or high seismic risk. Several studies, such as those by Leonhardt and Mönning (1975), Bazant *et al.* (1980), Aktan and Bertero (1980), Eberhard and Sozen (1993) among many others, expanded the knowledge of the shear resisting mechanisms and developed methods for determining the shear strength and detailing guidelines for ensuring adequate ductility. For a better understanding of the inelastic post-peak response of these structural elements several experiments on isolated panels under monotonic loading were conducted by Vecchio and Collins (1986), Bhide and Collins (1987), Pang and Hsu (1995). These were complemented by experiments on shear panels and shear walls under cyclic loading with significant inelastic strains by Stevens *et al.* (1987), Ohomori *et al.* (1989), Salonikios *et al.* (1999), Hidalgo *et al.* (2002), Thomsen and Wallace (2004), Mansour and Hsu (2005a), Greifenhagen and Lestuzzi (2005), Lowes *et al.* (2011), Turgeon *et al.* (2013), Ruggiero *et al.* (2016) among others.

In parallel with the experimental investigations, several finite element models have been proposed for describing the cyclic inelastic response of RC shear walls. These models fall roughly into two categories: (a) special purpose models of enhanced beam elements, and (b) general models based on plane stress or membrane finite elements.

Models of the first category refer, among others, to the fiber

beam elements for slender RC members by Martinelli and Filippou (2009), Mazars *et al.* (2006), Massone *et al.* (2006), Fischinger *et al.* (2004), Saritas and Filippou (2009), Jiang and Kurama (2010), Fischinger *et al.* (2012), Saritas and Filippou (2013), Beiraghi *et al.* (2015). These models are suitable for the simulation of large scale structures but are limited to cases of moderate shear demand, since they do not address all the shear resisting mechanisms of walls. Further studies are necessary for this type of models to enhance their performance in representing shear walls with complicated shear behavior Wu *et al.* (2016). The models of the second category usually follow the continuum approach where the effect of cracks (i.e., the discontinuity of the displacement field) is smeared within the element and the reinforcement bars are embedded in the element. According to such approaches a crack strain is defined in order to represent the crack opening. These models can be profitably used for complex plane stress conditions and thus they aim to be suitable for several types of RC structural elements, including shear panels. Thus the proposed model stands among this category. According to such an approach an appropriate constitutive law for concrete and reinforcement needs to be considered.

The concrete constitutive models of the second category often pursue the proposal of the equivalent uniaxial stress-strain relation by Darwin and Pecknold (1976) and its subsequent extensions with the modified compression field theory by Vecchio (1989, 1990), the non-linear elasticity Okamura and Maekawa (1991) the disturbed stress field model by Vecchio (2000) and the softened membrane model by Hsu and Zhu (2002), Mansour and Hsu (2005a). Moreover, general concrete constitutive models are sometimes used for the analysis of shear walls even if the authors did not define nor validate a RC membrane element Hofstetter and Mang (1995), FIB (2008).

Palermo and Vecchio (2007), Mo *et al.* (2008) have

*Corresponding author, Ph.D.

E-mail: diego.talledo@iuav.it

^aPh.D.

validated the smeared crack models with experimental results from RC panels and RC shear walls. These studies find relatively good ultimate strength agreement but suggest that further investigations on energy dissipation and deformation ductility are required. A limitation of these models is the lack of a multiaxial limit state surface and the need for parameter calibration for each type of specimen.

Three-dimensional constitutive models with scalar damage parameters offer a relatively simple and computationally efficient formulation for concrete, maintaining in the same time sufficient accuracy. Among the different options, elastic-damage models that neglect plastic deformations are suitable for practical engineering purposes because of their computational efficiency, but fail to capture the inelastic deformation accumulation under cyclic effects Faria *et al.* (2004). On the other hand, more sophisticated plastic-damage models give accurate results but often suffer from complexity and lack of computational efficiency. Furthermore, the extent of their validation against experimental results from RC elements under high shear is rather limited as recent investigations by Rhee *et al.* (2004), Krätzig and Pölling (2004), Cicekli *et al.* (2007) show. The few correlation studies for specimens under monotonic loading by Faria *et al.* (1998), Wu *et al.* (2006), Lee and Kuchma (2007) show good agreement with the use of two damage parameters, one under tensile and one under compressive stress states. The suitability of these constitutive models for the cyclic response simulation of RC shear walls is still under investigation.

The purpose of this study is the development of a computationally efficient membrane model for the simulation of RC structural elements under cyclic loads. The model aims to be general and, thus, suitable for several types of RC structural elements, while at the same time balancing accuracy with computational efficiency so as to be convenient for the earthquake analysis of large structural models. To meet these objectives the membrane element combines an innovative concrete constitutive law based on damage-plasticity and the embedded reinforcing bars neglecting the dowel action and the bond-slip effect.

2. Concrete constitutive relation

The proposed membrane model is based on a concrete constitutive relation with energy-based isotropic continuum damage. The model takes into account both tensile and compressive failure modes of concrete with two independent damage parameters, and also accounts for micro-crack opening and closing through the spectral decomposition of the effective stress tensor. The damage and plastic unloading/reloading processes are assumed to be elastic. The paper of Ju (1989) gives the detailed description of the elasto-plastic damage mechanics framework and the adopted notation. The decomposition of the total strain tensor into elastic strain $\boldsymbol{\varepsilon}_e$ and plastic strain $\boldsymbol{\varepsilon}_p$ contributions is a model basic hypothesis giving

$$\boldsymbol{\varepsilon} = \boldsymbol{\varepsilon}_e + \boldsymbol{\varepsilon}_p \quad (1)$$

The effective stress $\bar{\boldsymbol{\sigma}}$ is defined as the stress in a hypothetical state of deformation free of damage and in

tensor notation becomes

$$\bar{\boldsymbol{\sigma}} = \mathbf{C}_0 : \boldsymbol{\varepsilon}_e \quad (2)$$

where \mathbf{C}_0 is the fourth-order elastic stiffness tensor and $:$ indicates the tensor contraction over two indices. The locally averaged free energy potential Ψ is assumed as the sum of two elastic contributions Ψ_0^+ and Ψ_0^- related to the tensile and the compressive part of the effective stress tensor respectively and reduced by two independent damage parameters, according to Faria *et al.* (1998)

$$\begin{aligned} \Psi(\boldsymbol{\varepsilon}, \boldsymbol{\varepsilon}_p, d^+, d^-) &= \\ &= (1 - d^+) \Psi_0^+(\boldsymbol{\varepsilon}, \boldsymbol{\varepsilon}_p) + (1 - d^-) \Psi_0^-(\boldsymbol{\varepsilon}, \boldsymbol{\varepsilon}_p) = \\ &= (1 - d^+) \frac{1}{2} \bar{\boldsymbol{\sigma}}^+ : \boldsymbol{\varepsilon}_e + (1 - d^-) \frac{1}{2} \bar{\boldsymbol{\sigma}}^- : \boldsymbol{\varepsilon}_e = \\ &= \frac{1}{2} \bar{\boldsymbol{\sigma}} : (\mathbf{I} - \mathbf{D}) : \boldsymbol{\varepsilon}_e + (1 - d^-) \frac{1}{2} \bar{\boldsymbol{\sigma}}^- : \boldsymbol{\varepsilon}_e \end{aligned} \quad (3)$$

with d^+ representing the positive (tensile), d^- the negative (compressive) damage parameter and \mathbf{D} the fourth-order damage tensor that includes the spectral decomposition with the following expression, Wu *et al.* (2006)

$$\mathbf{D} = d^+ \mathbf{P}^+ + d^- \mathbf{P}^- \quad (4)$$

With \mathbf{P}^+ and \mathbf{P}^- the fourth-order positive and negative projection tensors, respectively

$$\mathbf{P}^+ = \sum_i H(\bar{\sigma}_i) (\mathbf{p}_i \otimes \mathbf{p}_i \otimes \mathbf{p}_i \otimes \mathbf{p}_i) \quad (5)$$

$$\mathbf{P}^- = \mathbf{I} - \mathbf{P}^+ \quad (6)$$

where H is the Heaviside step function, $\bar{\sigma}_i$ is the i -th principal stress of the effective stress tensor $\bar{\boldsymbol{\sigma}}$, \mathbf{p}_i stands for the corresponding principal stress direction and \otimes is the outer product symbol. The positive and negative part of the effective stress tensor, $\bar{\boldsymbol{\sigma}}^+$ and $\bar{\boldsymbol{\sigma}}^-$, respectively, can be determined from the projection tensors \mathbf{P}^+ and \mathbf{P}^- .

During a physical process the energy dissipation is non-negative in agreement with the first thermodynamic principle so that an admissible load-deformation process respects the following Clausius-Duhem inequality

$$\left(\boldsymbol{\sigma} - \frac{\partial \Psi}{\partial \boldsymbol{\varepsilon}} \right) : \dot{\boldsymbol{\varepsilon}} - \left(\frac{\partial \Psi}{\partial d^+} d^+ + \frac{\partial \Psi}{\partial d^-} d^- \right) - \frac{\partial \Psi}{\partial \boldsymbol{\varepsilon}_p} : \dot{\boldsymbol{\varepsilon}}_p \geq 0 \quad (7)$$

With the total strain as free variable the term in the first bracket should be always zero. This gives the relation between the Cauchy stress tensor $\boldsymbol{\sigma}$ and the effective stress tensor $\bar{\boldsymbol{\sigma}}$ that can be written as

$$\begin{aligned} \boldsymbol{\sigma} = \frac{\partial \Psi}{\partial \boldsymbol{\varepsilon}} &= \frac{\partial \Psi}{\partial \boldsymbol{\varepsilon}_e} = (1 - d^+) \frac{\partial \Psi_0^+}{\partial \boldsymbol{\varepsilon}_e} + (1 - d^-) \frac{\partial \Psi_0^-}{\partial \boldsymbol{\varepsilon}_e} = \\ &= (1 - d^+) \bar{\boldsymbol{\sigma}}^+ + (1 - d^-) \bar{\boldsymbol{\sigma}}^- = (\mathbf{I} - \mathbf{D}) : \bar{\boldsymbol{\sigma}} \end{aligned} \quad (8)$$

The second and third term of Eq. (7) provide the damage and the plastic dissipation inequalities, respectively. It can be proven that these quantities are always non-negative, e.g., Faria *et al.* (1998). The thermodynamic forces $Y^{+/-}$ conjugate to the damage variables, also called damage

energy release rates, are expressed as

$$\begin{aligned} Y^+ &= -\frac{\partial \Psi}{\partial d^+} = \Psi_0^+ \\ Y^- &= -\frac{\partial \Psi}{\partial d^-} = \Psi_0^- \end{aligned} \quad (9)$$

The damage energy release rates are used for the definition of the loading and unloading conditions of damage. The state of material damage is defined by a single damage criterion with the following quadratic functional form, Scotta *et al.* (2014)

$$g[\xi^+(Y^+), \xi^-(Y^-), r^+, r^-] = \left(\frac{\xi^+}{r^+}\right)^2 + \left(\frac{\xi^-}{r^-}\right)^2 - 1 \leq 0 \quad (10)$$

where ξ^+ and ξ^- are monotonically increasing scalar functions, and r^+ and r^- are the scalar damage thresholds monitoring the size of the damage surface in tension and compression, respectively. The inequality of Eq. (10) defines the elastic unloading/reloading domain and its closure is the damage surface at the incipient damage condition.

Furthermore, the expansion of the damage surface is determined by the evolution of the damage thresholds with the following flow rules

$$\begin{aligned} \dot{r}^+ &= \dot{\mu} \frac{\partial g}{\partial \xi^+} \\ \dot{r}^- &= \dot{\mu} \frac{\partial g}{\partial \xi^-} \end{aligned} \quad (11)$$

where μ is the damage consistency parameter. The Kuhn-Tucker conditions give

$$g \leq 0 \quad \dot{\mu} \geq 0 \quad \dot{\mu} g = 0 \quad (12)$$

while the consistency condition is

$$\dot{\mu} \dot{g} = 0 \quad (13)$$

The initial elastic domain for the virgin material is determined by the damage thresholds under uniaxial tension and compression, r_0^+ and r_0^- , respectively.

The evolution of the damage thresholds is computed with a predictor-corrector numerical scheme ensuring the computational efficiency of the material state determination process.

The quadratic form of the damage criterion ensures the independent evolution of the positive and negative damage thresholds for uniaxial tensile and compressive conditions, respectively. In fact, the partial derivatives of Eq. (11) are alternately zero when either ξ^+ or ξ^- is zero.

To characterize the damage criterion in Eq. (10), the monotonic functions ξ^+ and ξ^- are defined with the following equations according to previous studies, e.g., Berto *et al.* (2014)

$$\xi^+ = \sqrt{E_0(\bar{\sigma}^+ : \mathbf{C}_0^{-1} : \bar{\sigma}^+)} \quad (14)$$

$$\xi^- = \sqrt{3} \left(K \bar{I}_1^- + \sqrt{\bar{J}_2^-} \right) \quad (15)$$

where \bar{I}_1^- is the first invariant of $\bar{\sigma}^-$ and \bar{J}_2^- is the second

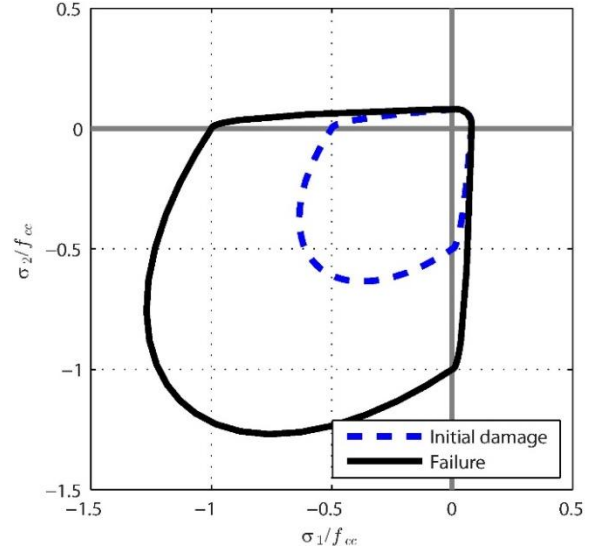


Fig. 1 Initial damage surface and failure envelope for plane stress conditions

invariant of the deviatoric part of $\bar{\sigma}^-$. E_0 is Young's concrete modulus and K a material parameter that accounts for the uniaxial compressive strength increase due to biaxial compression, Faria *et al.* (1998). Hence, the four parameters for determining the initial elastic domain are: r_0^+ , r_0^- , K , and the Poisson ratio ν . As discussed in detail in Faria *et al.* (1998), three common experimental tests are sufficient to establish the value of these parameters: a uniaxial tension test, a uniaxial and a biaxial compression test.

With Eq. (14) the initial positive damage threshold is equal to the concrete tensile strength, which describes the limit of the elastic domain for the constitutive stress-strain relation

$$r_0^+ = f_0^+ = f_{ct} \quad (16)$$

Since the compressive constitutive relation becomes nonlinear before reaching the peak strength, the uniaxial initial elastic limit f_0^- needs to be evaluated from the uniaxial compression test leading to the negative damage threshold from Eq. (15)

$$r_0^- = \frac{\sqrt{3}}{3} (K - \sqrt{2}) f_0^- \quad (17)$$

The results of a biaxial compression test permit the determination of the elastic limit $f_{0,2D}^-$ under biaxial compression. Thus, the parameter K which accounts for the increase of the compressive strength under a biaxial compression state can be determined from

$$K = \sqrt{2} \frac{f_{0,2D}^- - f_0^-}{2f_{0,2D}^- - f_0^-} \quad (18)$$

Fig. 1 shows the new initial damage surface in the space of normalized principal stresses for plane stress states.

A special feature of the proposed damage surface is the differentiation of the contribution of tensile and compressive damage processes in the description of the biaxial stress-strain response. This proves to be important

Table 1 Model parameters for compression tests

Parameter	Karsan and Jirsa (1969)	Kupfer <i>et al.</i> (1969)
f_{cc} (MPa)	23.5	32.5
E_0 (MPa)	31230	32500
ε_{cc}	1.56e-3	1.56e-3
f_0^-/f_{cc}	0.55	0.45
β	0.50	0.50
K	0.20	0.20

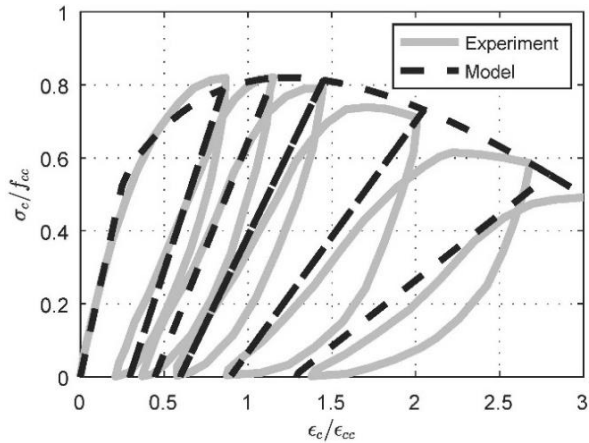


Fig. 2 1d cyclic compression experiment, Karsan and Jirsa (1969)

for the analysis of RC shear walls.

It can be readily verified that under pure compression ($Y^+ = 0$) the elastic domain simplifies to the modified Drucker-Prager criterion whose suitability in representing the biaxial stress response of concrete was confirmed in the studies by Lee and Fenves (1998), Faria *et al.* (1998), Wu *et al.* (2006).

The proposed constitutive model assumes that the damage criterion also describes the plastic surface so that the development of material damage is simultaneous with the accumulation of irreversible strains for all stress states.

Motivated by the proposal of Faria *et al.* (1998) for compressive stress states the following plastic evolution law is proposed for all stress states

$$\dot{\varepsilon}_p = \beta E_0 \frac{\langle \bar{\sigma} : \dot{\varepsilon} \rangle}{\langle \bar{\sigma} : \bar{\sigma} \rangle} (C_0^{-1} : \bar{\sigma}) \quad (19)$$

where β is the plastic strain coefficient. This choice leads to the direction of the plastic strain rate being parallel to the direction of the total strain rate.

It is clear that the proposed plastic strain evolution involves several simplifications relative to the “effective stress space plasticity” model used to couple the damage evolution with the plastic flow Ju (1989). In fact the plastic strain evolution law uses a constant plastic coefficient in place of the classical consistency parameter, and it assumes the coincidence of the “direction” of the plastic strain increment with the “direction” of the elastic strain. These simplifications are in the spirit of obtaining an efficient model for large scale seismic analyses without undue sacrifice of accuracy, as the correlation studies show. With

this assumption the coupling between damage and plasticity is simplified, eliminating additional iterations during the material state determination process. A consequent limitation of the model is the inaccurate representation of concrete dilatancy. In cases in which dilatancy plays an important role in the response of the structural element a different plastic potential should be used with the proposed constitutive model.

The evolution laws of the damage parameter d^+ and d^- of Eq. (3) identify the concrete constitutive behaviour. The following laws, inspired by the ones proposed by Faria *et al.* (1998), and modified by Berto *et al.* (2014), are used in this paper

$$d^+ = 1 - \frac{r_0^+}{r^+} \exp \left[A^+ \left(1 - \frac{r^+}{r_0^+} \right) \right] \quad (20)$$

$$d^- = 1 - \sqrt{\frac{r_0^-}{r^-}} (1 - A^-) - A^- \exp \left[B^- \left(1 - \sqrt{\frac{r^-}{r_0^-}} \right) \right] \quad (21)$$

where A^+ , A^- and B^- are positive parameters that can be set by specifying the fracture energy, the concrete compressive strength and the localized crushing energy according to Krätzig and Pölling (2004). Fig. 1 shows the resulting failure envelope in the space of normalized principal stresses for plane stress states.

3. Correlation studies of concrete material behavior

The following correlation of analytical with experimental results investigates the ability of the proposed concrete constitutive model to simulate the 1d and 2d behavior of plain concrete under tensile and compressive cyclic loading. The correlation studies also serve for the calibration of the plastic strain coefficient that is the only parameter that cannot be directly derived from common experimental tests on concrete specimens. Finally these studies validate the relation between the damage parameter and the progressive degradation of mechanical properties, Scotta *et al.* (2009), a subject that is beyond the scope of the present study but will be pursued in the future.

3.1 Uniaxial cyclic compression test

The correlation study for the cyclic uniaxial stress-strain response uses the specimen AC2-09 by Karsan and Jirsa (1969). The concrete compressive cylinder strength is $f_{cc} = 23.5$ MPa. The model parameters are listed in Table 1 where the symbol ε_{cc} stands for the concrete strain at the compressive cylinder strength.

Fig. 2 compares the numerical stress-strain response with the experimental measurements. The overall nonlinear behavior of the specimen is represented very well. The numerical envelope describes a linear elastic path followed by hardening and then softening response. The unloading and reloading branches show the progressive stiffness damage and the evolution of the plastic strain with the stiffness reduction related to the value of compressive damage and the residual strain depending on the plastic

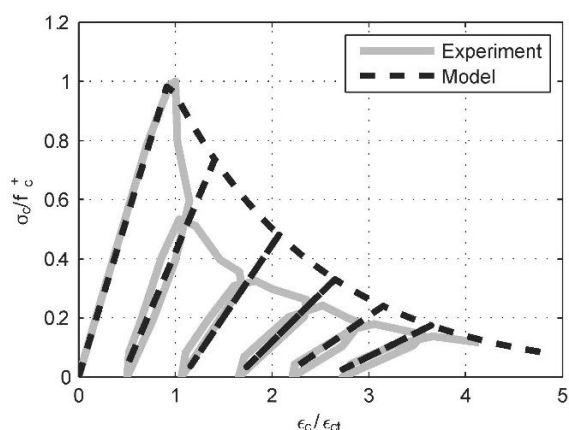


Fig. 3 1d cyclic tension experiment, Gopalaratnam and Shah (1985)

Table 2 Model parameters for tension test by Gopalaratnam and Shah (1985)

Parameter	Gopalaratnam and Shah (1985)
f_{ct} (MPa)	3.5
E_0 (MPa)	32000
ϵ_{ct}	1.56e-3
f_0^+ / f_{ct}	1.00
β	0.50

strain accumulation for each cycle.

The hysteresis of the reloading loop cannot be represented by the model because of the rate-independent elastic unloading/reloading assumption, but the progressive stiffness deterioration fits the experimental results well. The observed agreement proves sufficiently accurate for the simulation of concrete elements.

3.2 Uniaxial cyclic tension test

Fig. 3 compares the tensile response of the model with the experimental data by Gopalaratnam and Shah (1985). The tensile strength of concrete is $f_{ct} = 3.5$ MPa at the strain ϵ_{ct} . The material parameters are listed in Table 2. The stiffness deterioration and the residual strain at each unloading/reloading cycle agree well with the experimental results confirming the ability of the damage parameter and the plastic strain variable to capture the physical behavior.

The residual strains in tension are very important for the simulation of the cyclic local and global response of reinforced concrete membranes under shear, because they influence the crack closure at loading reversals. The exact representation of the post-peak tensile response of the plain concrete specimen is of secondary importance for the simulation of the average response of a reinforced concrete member over several cracks, particularly under the large inelastic deformations arising in earthquake engineering applications.

3.3 Uniaxial tension-compression with load reversal

Because the proposed concrete model is intended for

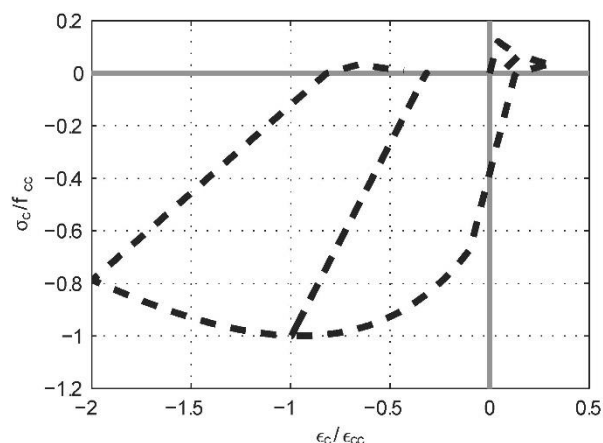


Fig. 4 1d cyclic tension experiment, Gopalaratnam and Shah (1985)

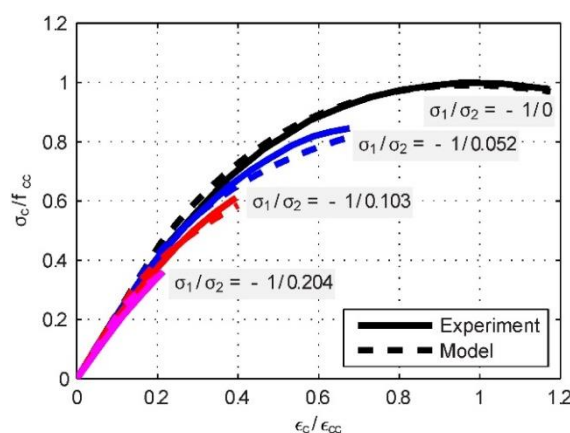


Fig. 5 Biaxial tension-compression with different stress ratios, Kupfer *et al.* (1969)

seismic response applications, its response in a uniaxial test with a more complex loading path consisting of two cycles in tension followed by two cycles in compression and concluding with a residual tensile stress is of interest. The concrete damage parameters are the same as for the uniaxial cyclic compression test. Fig. 4 shows that the model is able to account for crack opening, crack closing with stiffness recovery, and crack reopening. The evolution of the plastic strain and of the two damage variables determines the residual strain after unloading and the progressive stiffness deterioration in tension and in compression, respectively, as the stress-strain response in Fig. 4 shows.

3.4 Biaxial tension-compression tests

Four concrete cube specimens were subjected to different load conditions to failure by Kupfer *et al.* (1969). The third principal stress was kept equal to zero ($\sigma_3 = 0$) in all cases, while the other two principal stresses increased to failure with the following stress ratios: (1) $\sigma_1 / \sigma_2 = -1/0$, (2) $\sigma_1 / \sigma_2 = -1/0.052$, (3) $\sigma_1 / \sigma_2 = -1/0.103$ and (4) $\sigma_1 / \sigma_2 = -1/0.204$. The cylinder compressive strength is $f_{cc} = 32.5$ MPa. Fig. 5 compares the numerical response with the material parameters listed in Table 1 with the experimental results of the four specimens. The compressive strength

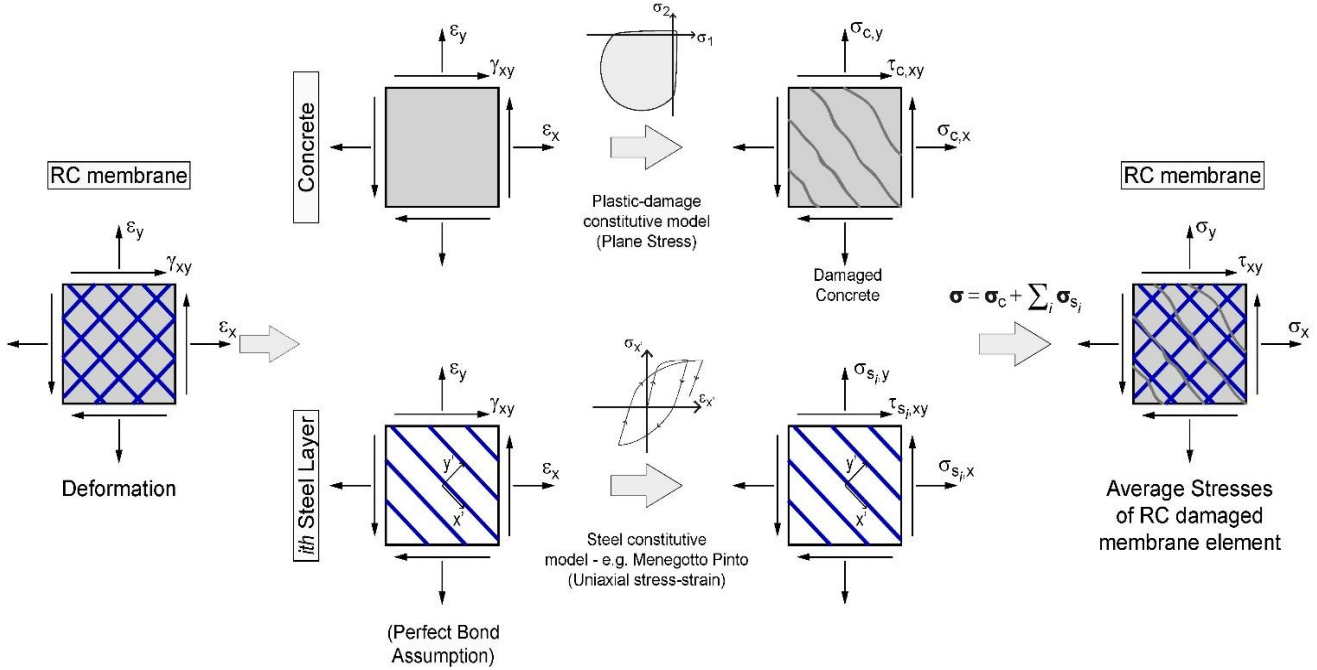


Fig. 6 Schematic representation of the membrane model for RC panels

reduction under different principal tension/compression ratios agrees well with the observed response for the proposed damage limit surface and its evolution law.

4. Membrane model for RC panels

The preceding concrete material model is implemented under plane stress states in a 4-node quadrilateral finite element. The plane stress implementation of the proposed model is straightforward and speeds up the material stress state determination in comparison with a 3D material formulation constrained for plane stress states. Following the embedded approach, the reinforcing bars with the same orientation are represented by an orthotropic steel layer that is superimposed on the concrete mesh assuming equivalence of strains. Thus perfect bond between reinforcing steel and concrete is considered in this work. Moreover such an approach offers computational efficiency for the large scale simulations envisaged for the proposed model. The exploration of the bond-slip effect on the panel behavior is left for a future study.

For a steel layer that represents one set of parallel reinforcing bars, the state determination starts with the projection of the generic total strain tensor $\boldsymbol{\epsilon}$ in the direction of the bars. With the direction cosines \mathbf{m} of the bar orientation the total strain of the steel bar is

$$\boldsymbol{\epsilon}_\phi = \mathbf{m} : \boldsymbol{\epsilon} : \mathbf{m} \quad (22)$$

The strain $\boldsymbol{\epsilon}_\phi$ gives the uniaxial steel stress σ_ϕ from the constitutive relation of the reinforcing steel. The proposed model uses the Menegotto-Pinto model with isotropic hardening for its ability to represent the hysteretic behavior of the reinforcing steel with good accuracy, Filippou *et al.* (1983), as long as reinforcing bar buckling is not significant. The material state in terms of the steel stress

Table 3 Model parameters for RC panel simulations

Parameter	Bhide and Collins (1987)	Mansour and Hsu (2005)	Stevens <i>et al.</i> (1991)
f_{cc} (MPa)	-23.0	-50.0	-23.0
ϵ_{cc} (%)	0.19	0.22	0.22
$f_{\bar{v}}/f_{cc}$	0.55	0.55	0.55
β	0.50	0.50	0.50
K	0.20	0.20	0.20

σ_ϕ and the tangent modulus C_ϕ is transformed from the reinforcement direction to the stress σ_s and tangent stiffness C_s in the original element reference frame with the following operations

$$\sigma_s = \sigma_\phi (\mathbf{m} \otimes \mathbf{m}) \quad (23)$$

$$\mathbf{C}_s = C_\phi (\mathbf{m} \otimes \mathbf{m} \otimes \mathbf{m} \otimes \mathbf{m}) \quad (24)$$

The contributions of the different steel layers are summed up and then added to the concrete contribution.

Fig. 6 illustrates schematically the proposed membrane model. The strains obtained from the nodal displacements of the finite element. As previously mentioned, assuming perfect bond, the same strains are considered for both concrete and each steel layer (in figure it is reported the i -th layer). The stress for concrete and each steel layer is evaluated with the proper constitutive law (the proposed plastic-damage model for concrete and Menegotto-Pinto model for each steel layer). Finally the average stress for the damaged RC membrane element is obtained by summing up the contributions of concrete and each steel layer as represented by the summation in Fig. 6.

5. Correlation studies of RC membrane model

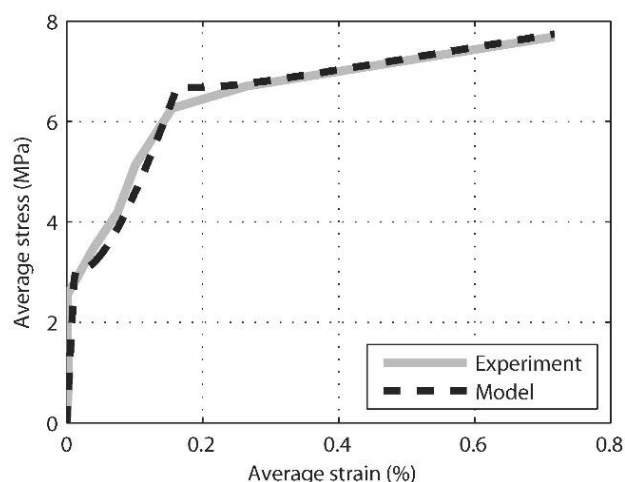


Fig. 7 Uniaxial tensile loading of RC panel by Bhide and Collins (1987)

In this section, correlation of numerical results with experimental data investigates the ability of the proposed RC membrane element to simulate monotonic and cyclic response of reinforced concrete panels subjected to uniform stress states. In particular the analysis of the membrane element in axial and shear actions applied in each direction independently is presented by using only one membrane element for each case. Then the coupling effect is investigated through the analysis of one membrane element subjected to combined axial and shear actions. The bending behavior of the membrane element as well as other problems related to non-uniform stress distribution will be treated in a future study.

5.1 RC panel under uniaxial tension

The first correlation study concerns the square RC panel with specimen number PB2 by Bhide and Collins (1987). The panel has side dimensions of 890 mm, thickness of 70 mm, and a reinforcing ratio of 2% in two orthogonal directions. The panel was subjected to monotonic uniaxial tension parallel to one reinforcing steel direction. The compressive cylinder strength is 23 MPa and the reinforcing steel has tensile yield strength of 240 MPa.

The panel is represented with one membrane element in the model with the parameters for the concrete model in Table 3. Fig. 7 shows the average stress versus average strain in the loading direction. It should be noted that the response in terms of average stress versus strain is a global measure, equivalent to a force versus displacement relation. The membrane model captures well the three phases of specimen behavior starting with the initial elastic response followed by concrete cracking, the yielding of the longitudinal reinforcement and finally its hardening response. Despite the perfect bond assumption between concrete and steel, the model results are closed to the experimental ones in the concrete cracking phase thanks to the fact that the uniaxial tension is parallel to one reinforcement direction and thanks to the calibration of the concrete constitutive law with the fracture energy in tension.

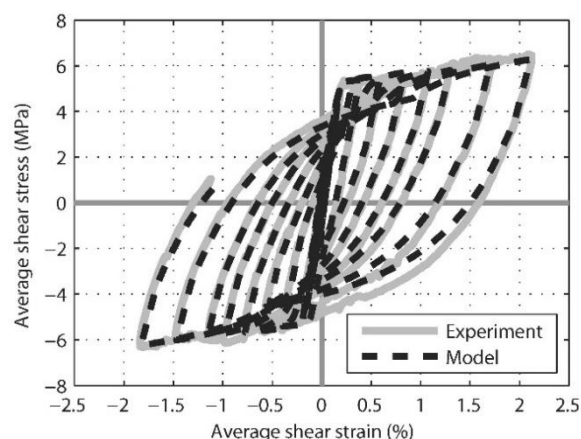


Fig. 8 Cyclic shear loading of RC panel by Mansour and Hsu (2005a)

Table 4 Mechanical properties of RC panels, Mansour and Hsu (2005a)

Panel	f_{cc} (MPa)	α	ρ_l	f_{yl} (MPa)	ρ_t	f_{yt} (MPa)
CA2	45	45.0°	0.0077	424.1	0.0077	424.1
CB3	48	45.0°	0.0170	425.4	0.0077	424.1
CD3	47	68.2°	0.0130	425.3	0.0130	425.4
CF2	44	79.8°	0.0056	424.1	0.0056	424.1
CE3	50	90.0°	0.0120	425.4	0.0120	425.4

5.2 RC panel under uniform cyclic shear

The second correlation study concerns the RC panel specimens of Mansour and Hsu (2005a). These specimens were 1397 mm square with a thickness of 178 mm and were reinforced with two orthogonal layers of steel reinforcement with different reinforcing ratios and different inclinations relative to the specimen's principal axes. The specimens were subjected to quasi-static, uniform cyclic shear at the panel mid-plane with monotonically increasing amplitude. The homogeneous stress state of pure shear at 45° to the horizontal was achieved by loading the panel edges with normal forces of equal value but opposite sign in two orthogonal directions. The specimens were subjected to cyclic load reversals, under load-control before the reaching of reinforcement yielding, and under displacement-control thereafter. During the test, the specimen strains were measured over a length crossing several cracks.

The specimens are divided in five groups CA, CB, CD, CE and CF, where the second letter refers to different reinforcement orientation. Each group is characterized by different specimens, labeled with different numbers, with different reinforcement ratios, for more details readers can refer to Mansour and Hsu (2005a). Table 4 gives the amount of reinforcement, its orientation and the mechanical properties of the constituent materials, with f_{cc} denoting the compressive cylinder strength, α the angle between the reinforcement in the longitudinal l -direction and the horizontal panel edge, ρ_l and f_{yl} the reinforcement ratio and the tensile yield strength of the bars in the l -direction, respectively, and ρ_t and f_{yt} the reinforcement ratio and

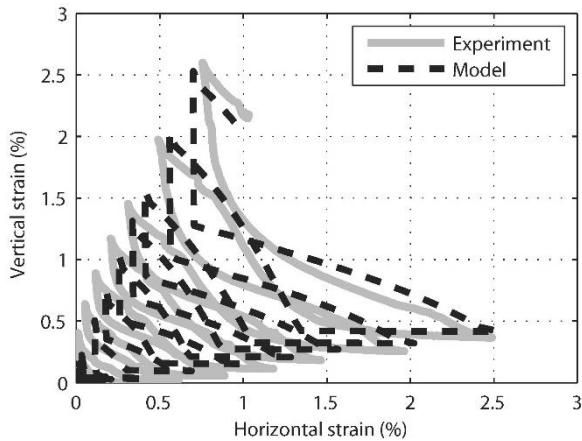


Fig. 9 Comparison of numerical results with measurements of vertical strain vs. horizontal strain for specimen CE3 of Mansour and Hsu (2005a)

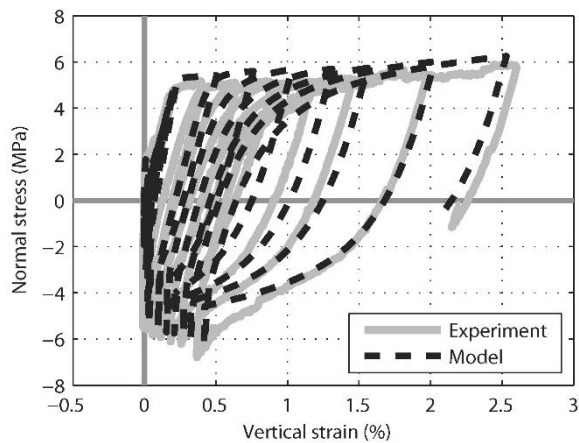


Fig. 10 Comparison of numerical results with measurements of normal stress vs. vertical strain for specimen CE3 of Mansour and Hsu (2005a)

the tensile yield strength of the bars in t -direction, respectively.

The complete collapse of specimens CA2 and CF2 could not be reached because of equipment limitations. The failure of specimens CB3 and CD3 was due to shear after the development of moderate or good deformation ductility, respectively.

Each specimen is represented with one membrane element in the model with the parameters for the concrete model in Table 3.

Fig. 8 compares the resulting numerical shear stress-strain response with the experimental measurements. The results show that the proposed model describes accurately several features of the measured panel response such as the initial stiffness, the cracked stiffness, the shear strength, the panel deformation ductility, the pinching of the hysteretic behavior, and the onset of concrete compression failure, where applicable.

To further assess the accuracy of the numerical model, the response of panel CE3 is compared with the measured vertical strain vs. horizontal strain relation in Fig. 9, and the vertical normal stress vs. corresponding vertical strain relation in Fig. 10. The agreement of the axial strains with

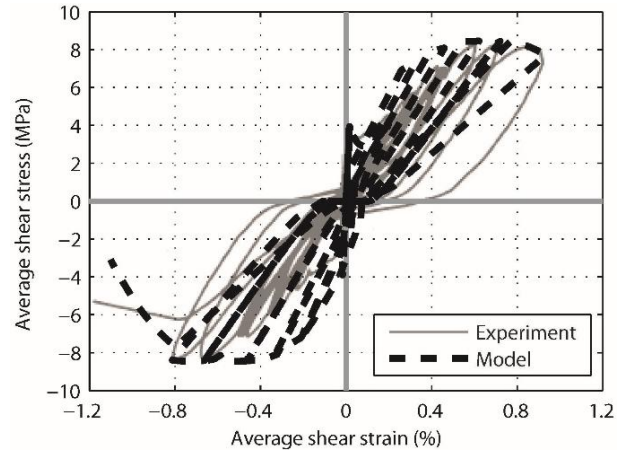


Fig. 11 Cyclic shear loading of RC panel by Stevens *et al.* (1987)

the experimental results is excellent. The progressive expansion of the panel due to the accumulation of plastic strains is captured very well by the proposed model. The slight discrepancy between experimental and analytical results at the sudden increase of compressive stress stems from the sudden closure of the cracks in the numerical model, which does not represent well the progressive stiffness recovery of rough crack closure in the specimen. This fact is also evident from the vertical vs. horizontal strain response in Fig. 9.

5.3 RC panel under compression with shear

The third correlation study concerns the square RC panel by Stevens *et al.* (1987) with side dimensions of 1625 mm and thickness of 285 mm. The reinforcing ratios were 2.93% and 0.98 in two orthogonal directions at 45° relative to the panel edges. The specimen for the correlation study identified as SE10 had compressive cylinder strength of 34 MPa and tensile yield strength for the reinforcing steel of 422 MPa and 479 MPa for the larger and smaller bar diameter, respectively. To induce a stress state of biaxial compression with shear the panel edges were subjected to normal stresses of opposite sign in the orthogonal directions with the compressive stress value equal to twice the value of the tensile stress. The specimen was subjected to cyclic load reversals under increasing deformation.

The specimen is represented with one membrane element in the model with the parameters for the concrete model in Table 3. Fig. 11 compares the numerical shear stress-strain relation with the average shear strain from the strain measurements at the panel edges. The results confirm the ability of the model to describe accurately several features of the measured panel behavior such as the yielding and subsequent hardening behavior, as well as the panel strength. The unloading stiffness and the residual strain are less accurate than those of the preceding example, because the direction of the reinforcing steel deviates from the loading direction and thus amplifies the effect of secondary shear resisting mechanisms in the RC panel. In fact, the cracks in the specimen are not parallel to the reinforcing mesh that might contribute to the shear strength not only

with axial tension but also through the dowel action. The significant effect of the dowel action on the unloading stiffness of the RC panel might arise from the fact that the reinforcing bars behave elastically upon load reversal. This limitation of the proposed membrane model will be further investigated in a future study.

5. Conclusions

The study describes a RC membrane element with a damage-plasticity model for the concrete in perfect bond with one or more biaxial orthotropic steel layers, each layer representing the reinforcing bars in two orthogonal directions. The concrete constitutive model couples damage with plasticity but avoids the internal iterations for the material state determination common in this type of formulation. While the consistent theoretical basis achieves robustness of the calculations, the lack of internal iterations improves significantly the numerical efficiency of the model and its suitability for large scale simulations. Key features of the proposed concrete constitutive relation are: a clearly defined multiaxial limit state function, two damage parameters with one describing the tensile damage state and one the compressive damage state, and an efficient plastic strain and damage evolution law for general three dimensional stress states.

The correlation studies with experimental results of concrete specimens under cyclic load conditions and single panels under uniform stress conditions lead to the following conclusions:

- The agreement of the model with measured data of the hysteretic response of concrete specimens confirm the model's ability to represent the nonlinear material behavior under uniaxial cyclic tension and compression, and biaxial stress states.

- The proposed RC membrane model is able to simulate the hysteretic behavior of RC panels with general reinforcement layout with satisfactory accuracy. The material constitutive relation for these studies is calibrated once against available material data and is used consistently in plane stress conditions without the need to further adjust the material parameters.

- The comparison of the numerical results with the experimental response measurements of single RC panels under uniform stress states confirm the model's ability to describe the shear strength and ductility of RC panels with sufficient accuracy.

More extensive correlation studies with specimens under complex stress conditions will be discussed in a future work.

Acknowledgments

The authors thank Professors T.T.C. Hsu and Y.L. Mo for providing the experimental data of RC panels tested at the Structural Research Laboratory of the University of Houston, Texas.

The authors express gratitude to Professor F.C. Filippou

for his valuable suggestions and comments.

References

- Aktan, A.E. and Bertero, V.V. (1985), "RC structural walls: Seismic design for shear", *J. Struct. Eng. ASCE*, **111**(8), 1775-1791.
- Bazant, Z.P., Tsubaki, T. and Belytschko, T.B. (1980), "Concrete reinforcing net: Safe design", *J. Struct. Div. ASCE*, **106**(9), 1899-1906.
- Beiraghi, H., Kheyroddin, A. and Kafi, M.A. (2015), "Nonlinear fiber element analysis of a reinforced concrete shear wall subjected to earthquake records", *Iran. J. Sci. Technol. Trans. Civil Eng.*, **39**(C2+), 409-422.
- Berto, L., Saetta, A., Scotta, R. and Talledo, D. (2014), "A coupled damage model for RC structures: Proposal for a frost deterioration model and enhancement of mixed tension domain", *Constr. Build. Mater.*, **65**, 310-320.
- Bhide, S.B. and Collins, M.P. (1987), *Reinforced Concrete Elements in Shear and Tension*, Department of Civil Engineering, University of Toronto, Canada.
- Cicekli, U.G., Voyiadjis, Z. and Abu Al-Rub, R.K. (2007), "A plasticity and anisotropic damage model for plain concrete", *J. Plast.*, **23**(10-11), 1874-1900.
- Darwin, D. and Pecknold, D.A. (1976), "Analysis of RC Shear Panels under Cyclic Loading", *J. Struct. Div. ASCE*, **102**(ST2), 355-369.
- Eberhard, M.O. and Sozen, M.A. (1993), "Behavior-based method to determine design shear in earthquake-resistant walls", *J. Struct. Eng. ASCE*, **119**(2), 619-640.
- Faria, R., Oliver, J. and Cervera, M. (1998), "A strain-based plastic viscous-damage model for massive concrete structures", *J. Sol. Struct.*, **35**(14), 1533-1558.
- Faria, R., Oliver, J. and Cervera, M. (2004), "Modeling material failure in concrete structures under cyclic actions", *J. Struct. Eng. ASCE*, **130**(12), 1997-2005.
- FIB Bull 45 (2008), *Practitioners' Guide to Finite Element Modeling of Reinforced Concrete Structures*, Fédération Internationale du Béton Bulletin, 45.
- Filippou, F.C., Popov, E.P. and Bertero, V.V. (1983), *Effects of Bond Deterioration on Hysteretic Behavior of Reinforced Concrete Joints*, Earthquake Engineering Research Center, University of California, U.S.A.
- Fischinger, M., Isaković, T. and Kante, P. (2004), "Implementation of a macro model to predict seismic response of RC structural walls", *Comput. Concrete*, **1**(2), 211-226.
- Fischinger, M., Rejec, K. and Isaković, T. (2012), "Modelling inelastic shear response of RC walls", *Proceedings of the 15th World Conference on Earthquake Engineering*, Lisbona, Portugal.
- Gopalaratnam, V.S. and Shah, S.P. (1985), "Softening response of plain concrete in direct tension", *ACI Struct. J.*, **82**(3), 310-323.
- Greifenhagen, C. and Lestuzzi, P. (2005), "Static cyclic tests on lightly reinforced concrete shear walls", *Eng. Struct.*, **27**(11), 1703-1712.
- Hidalgo, P.A., Ledezma, C.A. and Jordan, R.M. (2002), "Seismic behavior of squat reinforced concrete shear walls", *Earthq. Spectr.*, **18**(2), 287-308.
- Hofstetter, G. and Mang, H. (1995), *Computational Mechanics of Reinforced Concrete Structures*, Vieweg+Teubner Verlag, Wiesbaden, Germany.
- Hsu, T.T.C. and Zhu, R.R.H. (2002), "Softened membrane model for reinforced concrete elements in shear", *ACI Struct. J.*, **99**(4), 460-469.
- Jiang, H. and Kurama, Y.C. (2010), "Analytical modeling of medium-rise reinforced concrete shear walls", *ACI Struct. J.*

- 107(4), 400-410.
- Ju, J.W. (1989), "On energy-based coupled elastoplastic damage theories: Constitutive modeling and computational aspects", *J. Sol. Struct.*, **25**(7), 803-833.
- Karsan, I.D. and Jirsa, J.O. (1969), "Behavior of concrete under compressive loadings", *J. Struct. Div. ASCE*, **95**(ST12), 2543-2563.
- Krätzig, W.B. and Pölling, R. (2004), "An elasto-plastic damage model for reinforced concrete with minimum number of material parameters", *Comput. Struct.*, **82**(15-16), 1201-1215.
- Kupfer, H., Hilsdorf, H.K. and Rusch, H. (1969), "Behavior of concrete under biaxial stresses", *ACI J.*, **66**(8), 656-666.
- Lee, H.J. and Fenves, G.L. (1998), "A plastic damage concrete model for earthquake analysis of dams", *Earthq. Eng. Struct. D.*, **27**(9), 937-956.
- Lee, H.J. and Kuchma, D.A. (2007), "Seismic overstrength of shear walls in parking structures with flexible diaphragms", *J. Struct. Eng. ASCE*, **11**(1), 86-109.
- Leonhardt, F. and Mönnig, E. (1975), *Vorlesungen über Massivbau. Teil 2: Sonderfälle der Bemessung im Stahlbetonbau*, Springer Verlag, Berlin, Germany.
- Lowes, L.N., Lehman, D.L., Birely, A.C., Kuchma, D.A., Hart, C.R. and Marley, K.P. (2011), *UW-UIUC-UCLA NEESR Complex Wall Project: Summary of Planar Wall Test Program*.
- Mansour, M. and Hsu, T.T.C. (2005a), "Behavior of reinforced concrete elements under cyclic shear. I: Experiments", *J. Struct. Eng. ASCE*, **131**(1), 44-53.
- Martinelli, P. and Filippou, F.C. (2009), "Simulation of the shaking table test of a seven-story shear wall building", *Earthq. Eng. Struct. D.*, **38**(5), 587-607.
- Massone, L.M., Orakcal, K. and Wallace, J.W. (2006), *Shear-Flexure Interaction for Structural Walls*, ACI Special Publication-Deformation Capacity and Shear Strength of Reinforced Concrete Members Under Cyclic Loading, SP-236.
- Mazars, J., Kotronis, P., Ragueneau, F. and Casaux, G. (2006), "Using multifiber beams to account for shear and torsion. Applications to concrete structural elements", *Comput. Meth. Appl. M.*, **195**(52), 7264-7281.
- Mo, Y.L., Zhong, J. and Hsu, T.T.C. (2008), "Seismic simulation of RC wall-type structures", *Eng. Struct.*, **30**(11), 3167-3175.
- Ohomori, N., Tsubota, H., Inoue, N., Kurihara, K. and Watanabe, S. (1989), "Reinforced concrete membrane elements subjected to reversed cyclic in-plane shear stress", *Eng. Struct.*, **115**(1), 61-72.
- Okamura, H. and Maekawa, K. (1991), *Nonlinear Analysis and Constitutive Models of Reinforced Concrete*, Giho-do Press, Tokyo, Japan.
- Palermo, D. and Vecchio, F.J. (2007), "Simulation of cyclically loaded concrete structures based on the finite-element method", *J. Struct. Eng. ASCE*, **133**(5), 728-738.
- Pang, X.B.D. and Hsu, T.T.C. (1995), "Behavior of reinforced concrete membrane elements in shear", *ACI Struct. J.*, **96**(6), 665-677.
- Rhee, I., Willam, K.J. and Shing, B.P. (2004), *Dynamic Analysis of a Reinforced Concrete Structure Using Plasticity and Interface Damage Models*, Vail Cascade Resort, Vail Colorado, U.S.A.
- Ruggiero, D.M., Bentz, E.C., Calvi, G.M. and Collins, M.P. (2016), "Shear response under reversed cyclic loading", *ACI Struct. J.*, **113**(6), 1313-1324.
- Salonikios, T.N., Kappos, A.J., Tegos, I.A. and Penelis, G.G. (1999), "Behavior of reinforced concrete membrane elements in shear", *ACI Struct. J.*, **96**(4), 649-660.
- Saritas, A. and Filippou, F.C. (2009), "Inelastic axial-flexure-shear coupling in a mixed formulation beam finite element", *ACI Struct. J.*, **44**(8), 913-922.
- Saritas, A. and Filippou, F.C. (2013), "Analysis of RC walls with a mixed formulation frame finite element", *Comput. Concrete*, **12**(4), 919-936.
- Scotta, R., Talledo, D.A., Tesser, L. and Vitaliani, R. (2014), "Non-linear behaviour modelling of RC panels subjected to in-plane loads", *Proceedings of the 4th European Conference on Computational Mechanics*, Palais des Congrès, Paris, France, May.
- Scotta, R., Tesser, L., Vitaliani, R. and Saetta, A. (2009), "Global damage indexes for the seismic performance assessment of RC structures", *Earthq. Eng. Struct. D.*, **38**(8), 1027-1049.
- Stevens, N.J., Uzumeri, S.M. and Collins, M.P. (1987), *Analytical Modelling of Reinforced Concrete Subjected to Monotonic and Reversed Loadings*, Department of Civil Engineering, University of Toronto, Canada.
- Tesser, L., Filippou, F.C., Talledo, D.A., Scotta, R. and Vitaliani, R. (2011), "Nonlinear analysis of R/C panels by a two parameter concrete damage model", *Proceedings of the 3rd ECCOMAS Thematic Conference on Computational Methods in Structural Dynamics and Earthquake Engineering*, Corfu, Greece, May.
- Thomsen, J.H. and Wallace, J.W. (2004), "Displacement-based design of slender reinforced concrete structural walls-experimental verification", *J. Struct. Eng. ASCE*, **130**(4), 618-630.
- Turgeon, J., Hart, C., Marley, K., Birely, A., Lehman, D., Lowes, L. and Kuchma, D. (2013), *Seismic Behavior of Modern Reinforced Concrete Coupled Wall (Specimen CW1)*, Tech. Report, Network for Earthquake Engineering Simulation (NEES).
- Vecchio, F.J. (1989), "Nonlinear finite element analysis of reinforced concrete membranes", *ACI Struct. J.*, **86**(1), 26-35.
- Vecchio, F.J. (1990), "Reinforced concrete membrane element formulations", *J. Struct. Eng. ASCE*, **116**(3), 730-750.
- Vecchio, F.J. (2000), "Disturbed stress field model for reinforced concrete: Formulation", *J. Struct. Eng. ASCE*, **126**(9), 1070-1077.
- Vecchio, F.J. and Collins, M.P. (1986), "The modified compression field theory for reinforced concrete elements subjected to shear", *ACI Struct. J.*, **83**(2), 219-231.
- Wu, J.Y., Li, J. and Faria, R. (2006), "An energy release rate-based plastic-damage model for concrete", *J. Sol. Struct.*, **43**(3-4), 583-612.
- Wu, Y.T., Lan, T.Q., Xiao, Y. and Yang, Y.B. (2016), "Macro-modelling of reinforced concrete structural walls: State-of-the-art", *J. Earthq. Eng.*, 1-27.

HK